The Relationship Between DSCS III Sunlit Surface Charging and Geomagnetic Activity Indices

L. Habash Krause, B. K. Dichter, D. J. Knipp, and K. P. Ray

***Abstract*—The authors report on a survey of correlations between DSCS III satellite sunlit surface charging data and tabulated values of selected geomagnetic activity indices. This study is driven by the motivation to find a set of indices that have the potential to be used as proxies for determining the presence (nowcasting) and likely onset (forecasting) of surface charging. DSCS III data were compared with the Dst, ap, and the Polar Cap indices for a study period covering day 229, 1995 through day 115, 1999. Results show that: 1) significant correlations ($R^2 > 0.97$) between average frame charging level and all three geomagnetic activity indices exist, and 2) the probability of charging events increases monotonically with increasing levels of geomagnetic activity until extreme levels are approached. It is postulated that during these extreme geomagnetic events, an anomalous source of neutralizing ions may be present at geosynchronous orbit either due to direct input from the solar wind or to ion outflow from the ionosphere.**

I. Introduction

Charging of spacecraft in geosynchronous orbits has been the subject of investigations for over 30 years, beginning with the observations by instruments aboard the Advanced Technologies Satellite (ATS) 5 in the late 1960's and early 1970's [1]. It is important to understand spacecraft surface charging for the following reasons: 1) it is known to cause satellite operational anomalies [2]; 2) it affects the accuracy of certain diagnostic instrumentation, especially electrostatic analyzers built to provide *in situ* measurements of plasma parameters; and 3) it is known to accelerate the environmental degradation of sensitive materials (e.g., charging can cause enhancement of deposition onto optical surfaces [3]).

Spacecraft charging can appear in many forms, including frame (absolute) charging, which characterizes the frame-to-plasma potential difference, and differential charging, which characterizes frame-to-surface or inter-surface potential differences. Furthermore, due to the different discharge mechanisms and consequences following discharge, charging events are then sub-categorized depending on the depth of penetration of the electrons: electrons with energies greater than 100 keV are associated with deep dielectric charging [4], whereas electrons with energies in the range of several to several tens of keV are known to cause satellite surface charging [5]. The probability of a spacecraft experiencing a particular type of charging depends on the spacecraft materials, its exposure to sunlight, and the local plasma environment surrounding the spacecraft.

Manuscript received July 25, 2000. This work was supported in part by the U.S. Air Force Office of Scientific Research under Contract FO5611-95-D-0221 and by the National Science Foundation under Grant ATM 9613829.

L. Habash Krause and D. J. Knipp are with the Department of Physics, U.S. Air Force Academy, CO 80840 USA.

B. K. Dichter and K. P. Ray are with the Space Vehicles Directorate, Air Force Research Laboratory, Hanscom AFB, MA 01730 USA.

Publisher Item Identifier S 0018-9499(00)11250-X.

Since it is well known that geomagnetic activity leads to modification of the geosynchronous plasma environment, we seek a statistical relationship between charging event severity and geomagnetic activity. This study examines the frame surface charging observed during sunlight on the Defense Satellite and Communication System (DSCS) III and correlates the data with the values of the geomagnetic activity indices.

In order to devise and employ mitigation techniques to prevent or ameliorate charging effects, a solid understanding of the conditions that lead to charging is necessary. The ultimate goal is to develop a series of event nowcasting and forecasting tools by which autonomous spacecraft systems could methodically diagnose in real-time and predict with some lead-time surface charging events that may be considered a hazard or a nuisance to the mission. The first step was to associate the conditions of the local environment with observed charging events. Results from the Spacecraft Charging AT High Altitudes (SCATHA) P78-2 near-geosynchronous satellite mission demonstrate that the primary population of particles that instigates satellite surface charging is that of energetic electrons with energies in the 10's of keV range [5]. Using the SCATHA results, investigators were able to develop a surface charging diagnostic and mitigation experiment, appropriately called the Charge Control System (CCS), to fly on DSCS III. With the CCS, it was possible to determine the levels of frame charging and differential charging between the frame and two dielectrics representative of common spacecraft materials—kapton and astroquartz cloth. The CCS, explained in further detail in the following section, was launched in 1995 and is operational to this day. It is capable of determining levels of charging and using these levels as a trigger to activate a Xe plasma source to quench the charging events. Significant progress was made when the data from the CCS experiment were compared with the combined application of the Magnetospheric Specification and Forecasting Model (MSFM) [6] and a rigorous spacecraft charging model. An analysis of the results shows that the combined models accurately predict high-level ($V \geq 300$ V) spacecraft charging based upon the coinciding geomagnetic activity [7].

Now, with the examination of CCS data in this study, we take an empirical approach and search for geomagnetic indices that may serve as proxies for spacecraft sunlit frame charging events that may be taking place concurrently or in the near (~hours) future. The indices examined in this study include the Disturbance Storm Time (Dst) index, representing the activity of the magnetospheric ring current, the ap index, representing activity in the auroral ionosphere, and the Polar Cap Index (PCI), representing activity in the polar ionosphere. For the interested reader, a review of these indices is presented in [8].

The paper is organized as follows: The DSCS III satellite orbit and the CCS experiment is described in Section II. Then, observations of spacecraft sunlit frame charging as seen through ion spectra are presented in Section III. Also included in this section are the temporal histograms of charging occurrence that are indicative of event correlations with solar/geomagnetic activity. Section IV contains the statistical data and analysis of the correlation of the surface charging events with geomagnetic activity as represented by Dst, ap, and PCI. All data presented in this paper are for daylight intervals. Eclipse charging will be discussed in another paper. A discussion of the results appears in Section V, and the paper concludes with a brief summary in Section VI.

II. Mission Description

The CCS experiment resides on DSCS III, an operational, 3-axis stabilized geosynchronous satellite launched in August of 1995. A thorough description of the CCS program has been published previously [9], but a brief description of the system is presented here. The CCS consists of:

i) a Xe plasma generator
ii) an ion electrostatic analyzer (ESA) to measure ions in 31 differential channels between 17 eV and 12.3 keV for determining frame charging levels (one spectrum per 60 seconds)
iii) an electron ESA adapted to measure integral electron counts between 20 keV and 50 keV for determining the intensity of the frame charging electron population (one measurement per second)
iv) two surface potential monitors (SPM's), one with a Kapton blanket material and one with an Astroquartz material, for determining differential charging between the materials and vehicle ground (one measurement per 10 seconds)
v) a gas storage and control assembly with associated tank, valves and plumbing to provide the gas for the plasma generator
vi) a power electronics unit to control the gas assembly and plasma generator
vii) a microprocessor controller to detect the onset of adverse charging conditions and autonomously discharge the vehicle prior to excessive charge build-up.

The CCS autonomously detects hazardous differential charging conditions and actively protects the host spacecraft against the subsequent charging effects. It is capable of generating a Xe plasma in the spacecraft sheath within one minute of detecting differential charging above preset threshold values. The plasma source was allowed to operate for up to one hour per day. However, the observational components of the CCS, including the ion and electron ESA's and the two SPM's were operational at all Mission Local Times (MLT's).

III. Observations

An example of spacecraft charging and particle fluxes seen over a 24 hour period appears in Fig. 1. The data are for day 238 (25 August) of 1996, starting from midnight Universal Time (UT). Ion spectra, differential in energy (y-scale) and varying in time (x-scale), appear in the upper panel of the figure. The grayscale on the right of the panel applies to the log of the flux intensity of the ions. We determine the spacecraft frame charging from the peak in the ion spectra, using the principle that ions from the background plasma will be accelerated through the potential drop that exists between the charged body and the plasma [1]. In this example, the frame charging begins at a level of 50 V at approximately 27 000 seconds (07:31) UT, gradually increases to a peak value of 894 V at approximately 36 300 s (10:05) UT, then falls off to a value of 34 V at 43 700 s (12:08) UT.

The lower panel of Fig. 1 displays traces grayscale coded in the legend and described from top to bottom as follows: 1) 20–50 keV electron counts; 2) Astroquartz SPM1 Voltage; 3) Kapton SPM2 Voltage; 4) Xe plasma thruster on/off. The 20–50 keV electron count trace (black) shows an abrupt increase a half hour past midnight UT. Associated with the electron increase is the differential charging of the kapton SPM (red trace). Note that the Xe plasma source was activated during this differential charging event (starting at $\mathrm{UT} = 1800$ seconds), reducing the kapton SPM voltage close to background levels. Also note also that the electron count is elevated from UT $= 26\,000$ to $47\,000$ seconds—roughly the time spanning the frame charging duration.

The distribution of sunlit frame charging was measured as a function of local time and time of year for a study period covering day 229, 1995 through day 115, 1999. Each sunlit frame charging event was identified by the peak evident in the spectrogram of ion flux plotted against time and ion energy [1]. It is noted that, with the ion peak method, it is possible to miss charging events on occasion due to the field aligned motion of the ambient ions or due to a lack of ambient ions to be measured. For each day during which charging was observed, the total charging duration ($>$50 Volts), as well as the charging level averaged over each charging event and the maximum charging level during that day, were extracted from the ion data and recorded.

A histogram of sunlit frame charging data accumulated over the study period (Fig. 2) illustrates the frequency of the charging events and its dependence on local time. The observed local time dependence is similar to that observed during the SCATHA mission [9] and is well correlated with the intensity of ambient geosynchronous electrons with energies in the 10's of keV [10]. Indeed, Olsen [11] found that a threshold flux of charging electrons ($E \sim 10$ keV for ATS-6) was necessary to induce charging—even in eclipse.

The occurrence of sunlit frame charging over a period of one year is shown in Fig. 3. The 5-day running average of daily maximum charging level is dominated by structures with a period corresponding to one solar rotation. The 60-day running average, on the other hand displays well-defined maxima at the equinoxes and minima at the solstices. Both sets of features indicate the dependence of spacecraft charging on geomagnetic activity, as influenced by the sun. The 27-day periodic features, seen in the 5-day average, reflect the influence of the high-speed solar-wind streams on the magnetosphere. These streams are

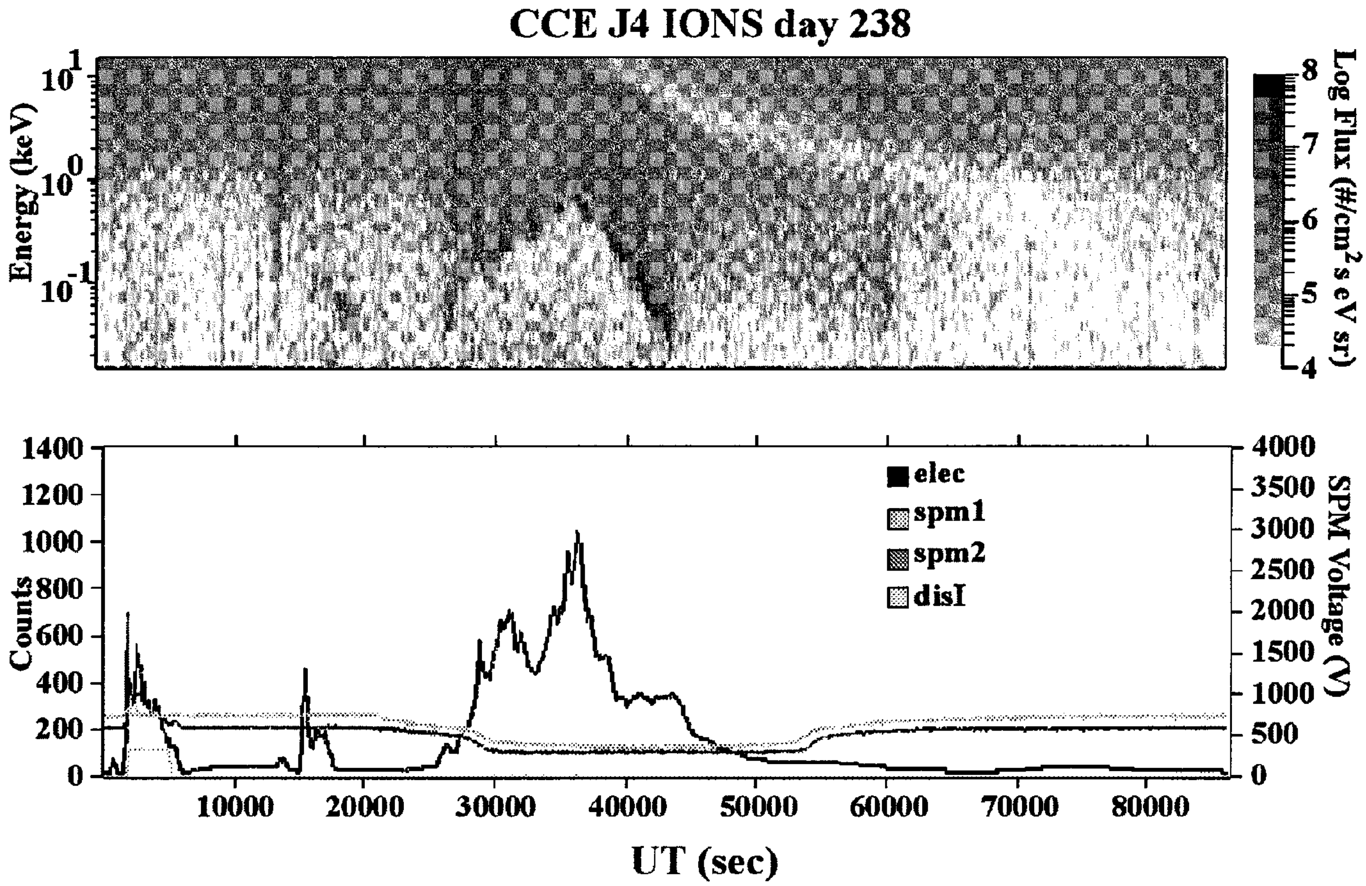

Fig. 1. DSCS III surface charging and particle observations appear over a 24 hour period, beginning at midnight UT. See text for details.

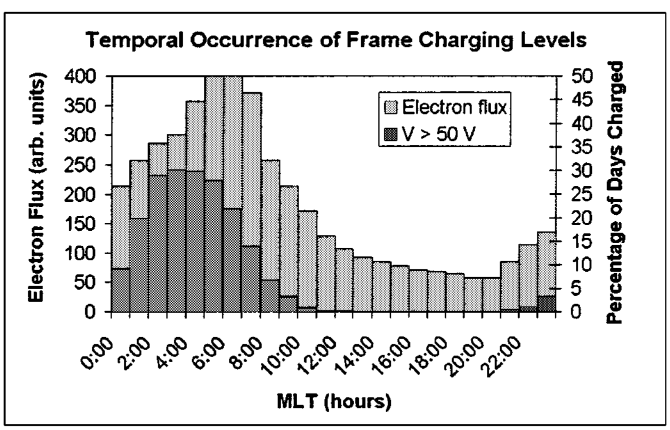

Fig. 2. Temporal distribution in MLT of various levels of frame charging for entire duration of charging study period. The primary y-axis denotes relative electron flux (arb. units), and the secondary y-axis denotes fraction of days at the corresponding MLT during which the frame charging levels were greater than 120 V.

emitted from regions of coronal holes on the sun and produce a fluctuating component of the interplanetary magnetic field, which is highly favorable for inducing geomagnetic activity. We note that 1996 was especially favorable for high speed streams; other years have a less pronounced 27 day signature.

Since there is a strong correlation between geomagnetic activity and solar/seasonal effects, the periodic features in our data provide us with hints that a statistically significant correlation can be found between spacecraft surface charging and geomagnetic activity.

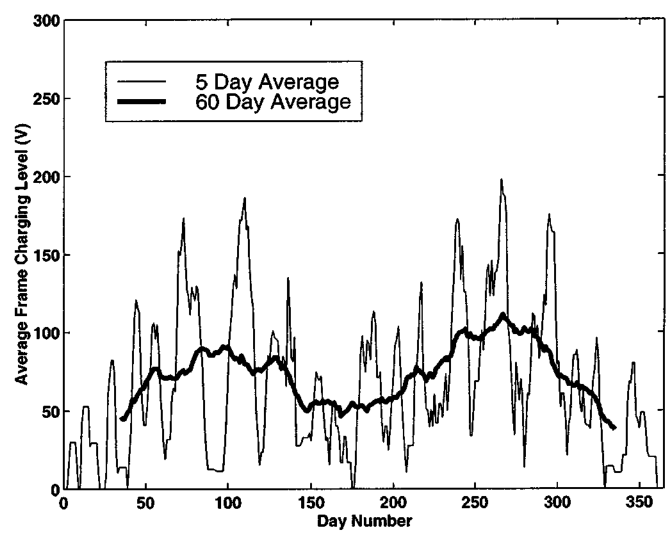

Fig. 3. Average daily frame potentials during 1996 are averaged over 5 day and 60 day periods, providing clear evidence of periodicity.

IV. Results

Two sets of charging statistics were computed for the geomagnetic activity parameters Dst, ap, and PCI. The first set, designed to test for the presence or absence of direct correlation, examines the day-to-day similarities between frame charging and different types of geomagnetic activity. The second set is designed to seek threshold levels of geomagnetic activity above which frame charging would be expected.

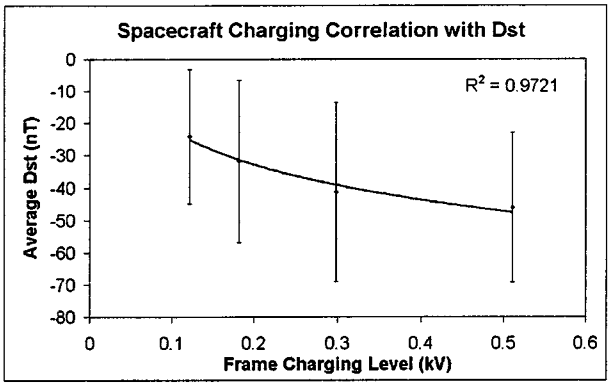

Fig. 4. Spacecraft charging correlation with average Dst.

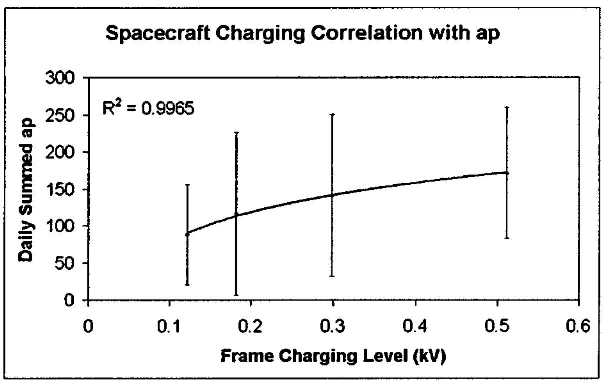

Fig. 5. Spacecraft charging correlation with daily summed ap.

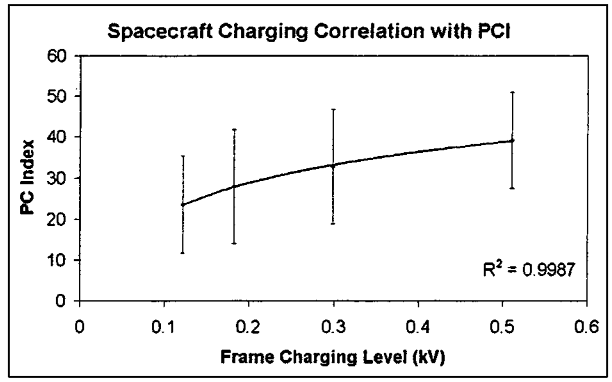

Fig. 6. Spacecraft charging correlation with daily summed PCI.

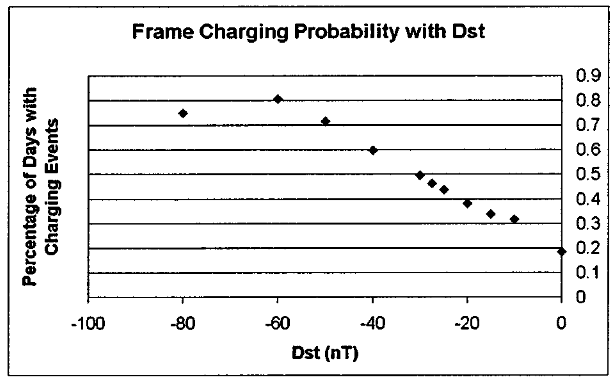

Fig. 7. Fraction of days that significant frame charging occurred as a function of average Dst.

First, direct daily correlations between the levels of frame charging V_f and geomagnetic activity were computed. Here, severity of charging for each day was determined by the level of charging maintained by the spacecraft for a minimum amount of time. Charging levels were divided into four bins: $50 > V_f > 120$ V, $120 > V_f > 240$ V, $240 > V_f > 460$ V, and $V_f > 460$ V. The minimum amount of time necessary for the spacecraft to have been considered charged at that level is 60 minutes for all thresholds except for a 10 minute period for the most extreme events ($V_f > 460$ V). Severity of ionospheric activity was determined by the 3-hour ap values and the hourly PCI values; each set of values was summed over each day, defined as 00:00 to 24:00 in UT. To represent severity of magnetospheric activity, Dst is averaged over the "prime charging time" interval during which spacecraft charging is considered to be most prevalent, specifically between 00:30 and 06:30 MLT. To simplify our analysis, only negative values of Dst (representing the main phase and recovery of a magnetic storm or substorm activity) and positive values of PCI (representing usual polar ionospheric convection) were considered.

Daily correlations of charging level versus geomagnetic activity for the three indices of interest appear in Figs. 4–6. Here, the charging level is defined as the average frame charging level within the bin under consideration. Fig. 4 shows the correlation for Dst, indicating a monotonic relationship between charging level and Dst averaged over the prime charging time. When a logarithmic fit is performed on the data, the Pearson correlation coefficient (R^2) between the mean charging level and Dst is found to be 0.972. Also shown on the plot are the bars representing the standard deviation from the mean Dst. Note that the variance is quite large, the consequences of which will be discussed in the next section. The correlation of daily charging with ap summed over each day appears in Fig. 5. Here, the correlation is even better, with a value of $R^2 = 0.996$ obtained from a logarithmic fit of the data. Similar results are found for the correlation of daily charging level with PCI summed over each day (Fig. 6), resulting in an R^2 of 0.999 associated with the logarithmic fit. Again, the variances as shown by the deviation bars are quite large and will be discussed in the next section.

The second set of statistics examines the fraction of days that DSCS charges significantly, defined here as $V_f > 50$ V for at least one hour continuously within the day, for a given level of geomagnetic activity. Levels of magnetospheric activity ranged from a Dst of -10 down to -80 nT, where an increase in the magnitude of the negative Dst signifies an increase inactivity. Similarly, values for daily summed ap and PCI ranged from 10 to 200 and 5 to 60, respectively.

The percentage of days during which the spacecraft was significantly charged was computed for threshold values of Dst averaged over prime charging time, daily summed ap, and daily summed PCI. Results appear in Figs. 7–9 An examination of Fig. 7 reveals a monotonically increasing charging probability with Dst magnitude until a peak of 80% is reached at approximately -60 nT. However, for greater magnitudes of Dst, there is actually a slight decrease in the charging probability with increasing activity—the spacecraft will only charge 75% of days with an average Dst of greater magnitude

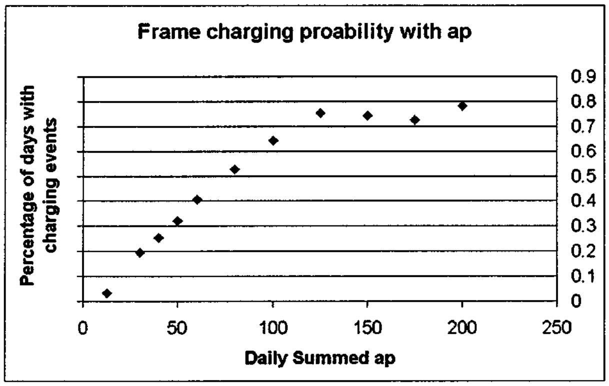

Fig. 8. Fraction of days that significant frame charging occurred as a function of the daily sum of ap.

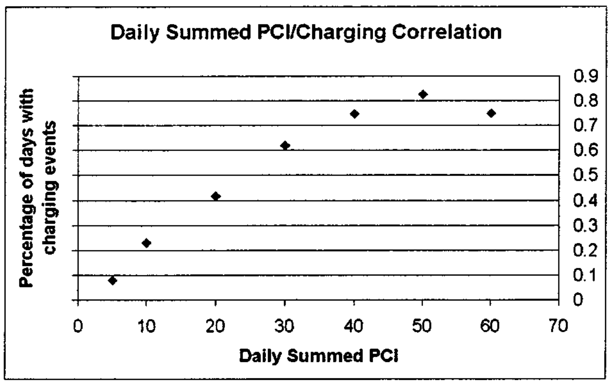

Fig. 9. Fraction of days that significant frame charging occurred as a function of the daily sum of PCI.

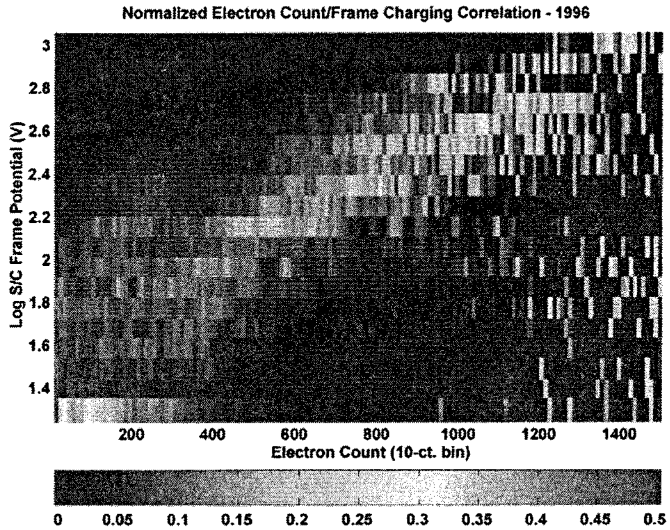

Fig. 10. Probability spectrogram of frame charging potential (y axis) correlated with incident electron ESA count rate (x axis). The gray scale bar indicates the relative fraction of events in which the measured electron count was associated with the corresponding frame potential. Each column is normalized so that the sum of the fractions for a given electron count is 1.

than 80 nT. The results for the ap threshold behave somewhat differently (Fig. 8). Again, the charging probability increases monotonically with summed ap up to a point (summed ap = 125), but then it decreases slightly with increasing activity before reaching extreme levels (summed ap = 200)—behavior that is indicative of a saturation effect. The PCI results behave more closely to the Dst results in that a peak in probability as a function of activity is reached, beyond which the probability of spacecraft charging actually decreases with increased activity (Fig. 9). Theories regarding this somewhat surprising behavior during extreme levels of geomagnetic activity and ramifications for nowcasting/forecasting systems will be presented in the following section.

V. Discussion

Two separate approaches were used to investigate the statistical relationship between DSCS III frame charging and various forms of geomagnetic activity. The method of direct daily correlations provides quantitative evidence that there is a significant ($R^2 \geq 0.97$) relationship between DSCS frame charging level and geomagnetic activity. Greater amounts of geomagnetic activity produce higher frame charging levels, a result that is consistent with the larger amount of charging electrons in the geosynchronous environment during periods of intense geomagnetic activity [12]. The plot of the observed charging intensity as a function of charging electron flux, as shown in Fig. 10, further illustrates this point. It is evident that there is roughly a monotonic relationship between charging electron count and spacecraft frame potential for the mid-range charging levels ($100 < V_f < 500$ V). However, the relationship is not as straightforward at low frame potentials, where perhaps lower energy electrons contribute more significantly to the determination of frame potential, and at high frame potential, where it appears to saturate at $V_f = 10^3$ V. This saturation effect may be due to spacecraft potential control by the photoelectrons. Since the photoelectron population is significantly more numerous than the other particle populations, the fact that any spacecraft charging occurs at all indicates that a large fraction of the photoelectrons is prevented from leaving the spacecraft. However, once a significantly large negative frame potential develops, the photoelectrons may be repelled from the spacecraft into the ambient plasma. Thus, no frame charging beyond some limiting negative voltage can develop regardless of the incident electron flux.

The second statistical method employed in our study examined the probability of significant spacecraft charging when the geomagnetic activity was measured to be above a wide range of threshold values. Here, the objective was to seek a way to specify minimum index values required for predicting the presence of significant charging and maximum values required to ensure absence of charging. Intuitively, we would expect that an increase in geomagnetic activity would produce a greater probability in significant spacecraft charging, and for low to moderate levels of geomagnetic activity, our results support this. However, when extreme levels of geomagnetic activity are considered, the probability saturates with increasing levels of geomagnetic activity. Similar results were found in a study that computed the probability of electrostatic discharge associated with surface charging as a function of geomagnetic activity [13]. This saturation effect can be explained by the presence of unusual geophysical processes associated with the extreme events that result in extraordinary modification of the geosynchronous environment. We consider the possibility of unusual modifications in three particle populations that would result in negation of spacecraft charging: 1) a depletion of charging electrons, resulting in an electron environment that is below the threshold necessary for charging; 2) a large flux of low energy electrons, resulting in large amounts of secondary electrons which are able to escape the spacecraft sheath, providing a positive source of current to neutralize the spacecraft; and 3) a large flux of ions, again providing a positive source of current for neutralization. No comments may be made regarding the low energy electrons since DSCS III does not have instrumentation necessary to measure these. However, we can look at the other two options. A survey of the data reveals that during the seven most extreme events (with a prime time Dst ranging from -85 to -241 nT) when charging was not observed, five of these days had a significant population of charging electrons and an excess of ions of densities up to two orders of magnitude over the background. For comparison, we note that the excess ions were observed in only three out of 28 extreme geomagnetic events accompanied by charging. An absence of charging electrons was observed during only one extreme event absent of charging.

The conclusion is that during extreme levels of geomagnetic activity, there is a finite probability that geophysical processes will lead to enhanced fluxes of ions in the geosynchronous environment that could significantly mitigate spacecraft charging events. An example of such a process may be the ion outflow of ionospheric sources that are most often associated with magnetic storms [14]. Since the magnetic storms are more prevalent and severe during periods of solar maximum, we could, in principle, test this theory by observing the behavior of the charging probability versus activity level as a function of position in the solar cycle. In addition, it has been shown that some geomagnetic activity indices respond differently to different types of solar wind (e.g., coronal mass ejections versus high speed streams) [15], so perhaps a combination of parameters would provide more information on how the geosynchronous environment responds to extreme levels of activity—thus providing a more accurate specification of charging probability. We suggest these topics would be of interest for future work.

An alternate explanation for the absence of charging during periods of extreme geomagnetic activity is that differential charging may create potential wells that prevent photoelectrons from escaping the spacecraft sheath. A detailed model of the spacecraft and charging environment would be necessary to investigate this possibility, and charging simulations may be accomplished with sophisticated numerical models, such as NASCAP-2K. This is another topic for future study.

The large variances in the direct daily correlations make it impractical to set specific thresholds in geomagnetic activity to definitively nowcast the presence or absence of spacecraft charging. However, we can say that for the DSCS III spacecraft, if any of the following three conditions are true, there is roughly a 75% chance that the spacecraft experienced significant charging: 1) the average Dst (averaged over the time period of 00:30–06:30 MLT) is negative and has a magnitude greater than 50 nT; 2) the daily summed ap is greater than 125, or 3) the daily summed positive PCI is greater than 40. In this sense, it has been demonstrated that an activity threshold for a significant fraction of charging events can be determined.

In closing, we note that from the point of view of spacecraft operators, a computed index that predicts charging probability and severity is of significant value, even if the predictions are statistical in nature. The next step is to investigate the possibility of relating the charging probability to solar wind parameters (measured at L1) and other solar activities that could provide advance warning. We intend to continue our work with the DSCS III CCS data to explore these issues.

VI. Summary

This study provides the next progressive step in the development of a real-time forecasting/nowcasting system presently in demand by the space science, engineering, and operations communities. It has been shown that a solid correlation exists between levels of geomagnetic activity (represented by the indices Dst, ap, and PCI) and levels of DSCS III frame charging in geosynchronous orbit. In addition, the probability that the spacecraft will significantly charge increases with geomagnetic activity until extreme levels of activity are reached. During these times, unusual geophysical processes may result in an anomalously large population of ions in the geosynchronous environment, providing a neutralizing source of positive current to the spacecraft. Suggestions for future work include a detailed investigation of the charging environment during extreme events, extension of this survey to cover as much of a complete solar cycle as possible, and investigation of a correlation between charging events and solar wind parameters as measured at L1.

Acknowledgment

The authors wish to express their gratitude to M. S. Gussenhoven for her insights and valuable contributions to the preparation of this manuscript.

References

[1] S. E. DeForest, "Spacecraft charging at synchronous orbit," *J. Geophys. Res.*, vol. 77, p. 651, 1972.
[2] C. F. Hoeber, E. A. Robertson, I. Katz, V. A. Davis, and D. B. Snyder, "Solar array augmented electrostatic discharge in GEO," in *17th International Communications Satellite Systems Conference and Exhibit*, 1998, AIAA-98-1401.
[3] D. P. Cauffman, "Ionization and attraction of neutral molecules to a charged spacecraft,", SAMSO TR-73-263, 1973.
[4] I. Katz, M. Mandell, G. Jongeward, and M. S. Gussenhoven, "The importance of accurate secondary electron yields in modeling spacecraft charging," *J. Geophys. Res.*, vol. 91, no. A12, p. 13 739, 1986.
[5] E. G. Mullen, M. S. Gussenhoven, D. A. Hardy, T. A. Aggson, B. G. Ledley, and E. Whipple, "SCATHA survey of high-level spacecraft charging in sunlight," *J. Geophys. Res.*, vol. 91, no. A2, p. 1474, Feb. 1986.
[6] J. Freeman and A. Nagai, "1993, The magnetospheric specification and forecast model: Moving from real-time to prediction," in *Solar-Terrestrial Predictions—IV Proceedings of a Workshop at Ottawa*, Canada, May 18–22, 1992.
[7] I. Katz, V. A. Davis, M. Mandell, D. Cooke, R. Hilmer, and L. Habash Krause, "Forecasting satellite charging: Combining space weather and spacecraft charging," , Jan. 2000, AIAA-2000-0369.
[8] M. G. Kivelson and C. T. Russell, *Introduction to Space Physics*: Cambridge, 1995.

[9] E. G. Mullen *et al.*, "An autonomous charge control system at geosynchronous altitude: Flight results for spacecraft design considerations," *IEEE Trans. Nucl. Sci.*, vol. 44, p. 2188, Dec. 1997.

[10] H. B. Garrett *et al.*, "Modeling of the geosynchronous plasma environment—Part 2, ATS 5 and ATS 6 statistical atlas,", AFGL-TR-78-0304, 1978.

[11] R. C. Olsen, "A threshold effect for spacecraft charging," *J. Geophys. Res.*, vol. 88, no. A1, p. 493, Jan. 1983.

[12] T. W. Lezniak and J. R. Winckler, "Experimental study of magnetospheric motions and the acceleration of energetic electrons during substorms," *J. Geophys. Res.*, vol. 75, p. 7075, 1970.

[13] G. L. Wrenn and R. J. K. Smith, "Probability factors governing ESD effects in geosynchronous orbit," *IEEE Trans. Nucl. Sci.*, vol. 43, Dec. 1996.

[14] I. A. Daglis, "The role of magnetosphere-ionosphere coupling in magnetic storm dynamics," *Geophys. Monogr.*, vol. 98, p. 107, 1997.

[15] D. J. Knipp and L. H. Krause, "Statistical survey of geoeffectiveness of solar wind structures in exciting the ionosphere and magnetosphere," in *Geospace Environment Modeling Workshop*, Snowmass, CO, 2000.